RESIDUAL STRESSES IN RAILWAY WHEELS AND THEIR EFFECT ON DAMAGE RATES THROUGH THE LIFE OF A WHEEL

Paul Molyneux-Berry, Adam Bevan
University of Huddersfield, Queensgate, Huddersfield HD1 3DH, UK

ABSTRACT

Wheelset maintenance and renewal comprises a significant portion of the whole-life cost of railway rolling stock. At present, many GB passenger trains have their wheels turned on a lathe at regular intervals to prevent the propagation of Rolling Contact Fatigue (RCF) cracks in the rim. Evidence from a number of fleets suggests that RCF damage occurs much more quickly as the wheelsets near the end of their life.

Wheel manufacturing processes are intended to induce a compressive hoop stress in the wheel rim to reduce crack propagation rates. Variations in residual stress through the life of a wheel may potentially influence the observed damage rates. This paper describes an experiment to measure residual stresses in new and used wheel rims to identify whether this could be a significant factor.

Assuming that the as-manufactured stress distribution was similar for all three wheels, it is found that the stresses are redistributed within the wheel rim during its life as material is removed and plastic flow occurs. However, the hoop stress near the running surface remains compressive.

Keywords: Railway Wheel Neutron Diffraction Residual Stress

BACKGROUND

Rolling Contact Fatigue in Railway Wheels

Railway wheels operate in a demanding environment with high normal contact forces and significant tangential forces. The resulting stresses often exceed the yield stress of the as-manufactured wheel material, leading to plastic flow, wear and fatigue damage. Wheelset maintenance and renewal comprises a significant portion of the whole-life cost of railway rolling stock.

In a recent survey of wheel damage on over 90% of UK passenger fleets, rolling contact fatigue (RCF) was found to be a dominant damage mechanism [1] and many fleets have their wheels turned on a preventive distance-interval basis to control the depth of RCF cracks. The types and locations of RCF damage have been monitored and related to the operating conditions of the fleet [2].

However, the current ‘state of the art’ for modelling of RCF damage in railway wheels has not achieved an integrated deterministic model of wheel damage owing to the complexity of the conditions [3],[4],[5]. The authors of this paper are researching the influences of the manufacturing and maintenance processes and the operating conditions on the nature and severity of RCF crack growth.

Railway Wheel Manufacturing Overview

Modern multiple-unit trains running in the UK are fitted with one-piece forged wheels, usually to the rim-chilled hypoeutectoid grade known as R8T or ER8T. The chemical composition and properties of the steel are tightly defined by the relevant national and international standards [6], [7].

The manufacturing process for these wheels is complex [8], and also well described in online literature [9], [10]. After rough machining, the wheel is heated to approximately 900°C (austenitisation) and the wheel rim (only) is then rapidly water quenched to 300°C. The wheel is then left to slowly air-cool. This process achieves two key goals:

- The rapid rim quenching makes the wheel rim material harder than the wheel centre, and thus more resistant to wear and crack initiation. Meanwhile the wheel web and centre are softer and therefore less prone to crack propagation.
- The slow contraction of the web and centre during air-cooling causes compressive residual hoop stresses in the already-hardened wheel rim, thereby making it more resistant to crack propagation. Meanwhile the wheel web and the inner part of the rim carry residual tensile stresses.

RCF CRACK GROWTH RATES

Many factors influence the growth rate of RCF cracks in wheels, including the train type, operating and environmental conditions and the position of a wheelset in the train [1]. The experience of maintainers on several GB rolling stock fleets suggests that RCF damage occurs much more quickly as the wheelsets near the end of their life (i.e. approaching the minimum diameter before the wheelset is renewed). Figure 1 shows examples of this trend for a fleet monitored by the authors; wheels turned for other reasons (e.g. flats, wear) are excluded. The authors suggest a number of possible reasons for this effect, as listed in Table 1.

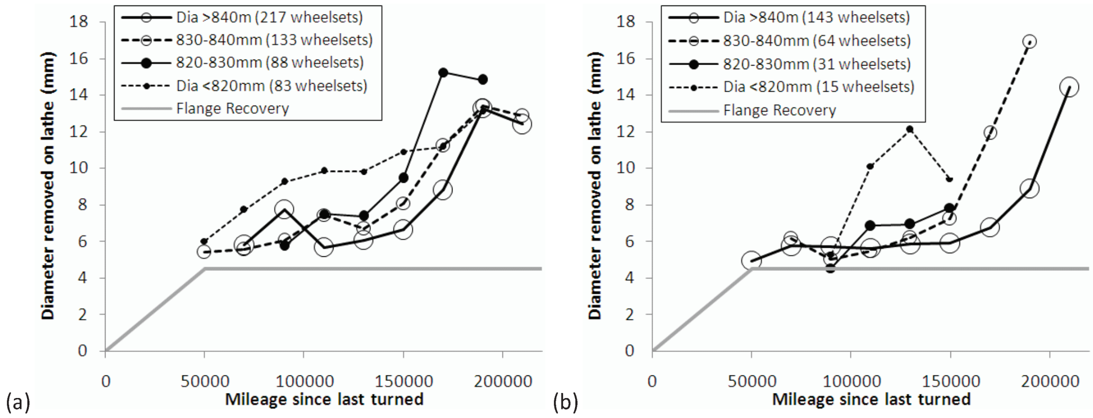

Figure 1: Wheel diameter lost at turning (reprofiling on a lathe) to remove RCF-cracked material, for a UK multiple-unit fleet. This shows the influence of wheel diameter: for a given mileage run, the cracks have propagated more deeply on smaller diameter wheels so the diameter loss is greater – (a) shows all wheels turned over a six-year period, (b) shows data for wheels made by one manufacturer. It is necessary to remove approximately 5mm to restore the wheel flange shape even when no cracks are present.

Table 1: Possible reasons why RCF crack propagation is faster on end-of-life wheels (smaller diameter)

Possible Reason	**Comment**
Change in material properties (hardness, microstructure) with depth below the as-manufactured tread surface	This has been investigated by the authors [5] and is believed to be significant.
Reduction in residual compressive stress remaining from the manufacturing process (beneficial compressive hoop stresses at the surface are lost due to plastic flow, wear and material removal at reprofiling).	Variations in residual stress have been measured [11], [12] and some models have considered their influence on RCF damage [4], which may be significant.
Increased contact stress (due to smaller wheel radius).	The change in wheel diameter is ≈6% which would increase the Hertzian contact stress by ≈2%; while this may be a contributory factor it is probably not sufficient to be the sole cause.
Higher number of stress cycles for a given wheelset mileage (due to increase in number of wheel revolutions).	The change in revolutions/mile is ≈6%; while this may be a contributory factor Figure 1 indicates that this is insufficient to be the sole cause.
Reduced wheelset rolling inertia increasing the probability of wheel spin or slide events. These cause thermal damage which can accelerate crack initiation or propagation	On the monitored fleet, improvements in the wheel slide protection and traction control software have reduced the occurrence of these events, and they are excluded from the data presented in Figure 1. However, they may be a contributory factor on some fleets.
'Human factors' issues: in an attempt to prolong wheel life, the lathe operator may minimise the cut depth on a small wheel, and thereby not remove all previous damage.	This has been identified as a problem on some fleets, and may be relevant but is difficult to assess and quantify. Considering the experience of the staff at the depot and the detailed monitoring undertaken by the authors, this is unlikely to have a significant influence on the monitored fleet.

This paper outlines experiments to investigate changes in residual stress through the life of a wheel, with a view to identifying whether this could contribute to the observed crack propagation rates. Four wheels were used for the tests. All wheels were manufactured to the same design by the same manufacturer, for use on the fleet of trains showing the trends illustrated in Figure 1.

One new wheel of Ø851mm was never fitted to an axle or used. Two mid-life wheels of Ø831mm were removed from service after 389,000 miles and had been turned twice. These ran on the same bogie and had an identical history: one of these was sectioned to provide stress-free samples. One end-of-life wheel of Ø796mm was acquired after removal from service: this ran on the same train as the mid-life wheels but had been fitted earlier, running 686,000 miles and being turned four times. All three used wheels had run 132,000 miles since they were last turned/reprofiled on the lathe.

MEASURING RESIDUAL STRESSES IN WHEELS

Selection of Techniques

Many techniques are available for measuring residual stresses or strains, but not many can be effectively applied to large solid steel components such as railway wheels. The significant residual stresses in a wheel are relaxed by cutting operations, so it is usually necessary to test an entire wheel, which is typically 900mm in diameter and has a mass of 400kg. Table 2 lists some methods which can be applied to wheels in practice.

Considering these methods, it was decided to use the simple ultrasonic bi-refringence method on several wheels, and then to test a sub-set of these using neutron diffraction. Starting with non-destructive methods allows the possibility of subsequent destructive tests on the same samples for comparison purposes.

After completion of the ultrasonic testing, one wheel required sectioning to provide stress-free reference samples for the neutron diffraction measurements. An initial radial cut was made to evaluate the simplest of the destructive techniques, and to gain experience in EDM cutting of entire wheels for a possible future application of the contour method [13].

Table 2: Methods for measuring residual stresses or strains in railway wheels

Method	Type	Notes
Radial cut, measure closing of gap	Destructive	Defined in UK standards [6]. Simple to carry out but limited information obtained.
Strain-gauging of segment followed by progressive material removal	Destructive	Defined in EN standards [7]. More complex method but only provides a general overview of residual strains.
Contour method: accurate co-ordinate measuring of a cut surface to determine which parts have bulged when stress is released	Destructive	Can provide very good stress distribution across the cut surface [13]. Relies on a very high quality smooth EDM cut which is difficult to achieve with the size and cross-section of a wheel, which also tends to close up the cut faces and trap the EDM wire
Ultrasonic bi-refringence techniques [12]	NDT	Commercially available and portable but provides only an indirect measure of strain averaged through the wheel rim width. May be used for manufacturing quality control [7] and failure investigations.
Neutron Diffraction	NDT	Can measure 3D strain field a small 'gauge volume' within the bulk of a sample several centimetres thick [11]. Limited beamtime available, few facilities can handle large/heavy samples.
Finite Element Analysis (FEA) in conjunction with another method	N/A	FEA of manufacturing processes [14],[15] can predict stress distributions, which can be compared to limited measurements from other methods described above. FEA can also be used in conjunction with sectioning methods to improve the resolution of results. However, FEA of the inhomogeneous, anisotropic, plastically flowed and cracked material near the running surface of the wheel is difficult.

NEUTRON DIFFRACTION MEASUREMENT OF RESIDUAL STRESSES

Previous Work

Neutron diffraction is a non-destructive technique for accurate measurements of residual strains and stresses, and offers the capability to measure strains in a small 'gauge volume' within the bulk of a large sample [11]. Several researchers have measured residual strains in railway wheels using neutron diffraction techniques. These have focused on the stresses of newly manufactured wheels [11],[18] and the influence of running on radial strains [19], but only near the running surface of the wheel. In the existing literature there is no publication describing neutron diffraction measurements of hoop strain in wheels that have run in service, nor of wheels that have had material removed by turning.

Methodology: Wheel Configuration

The measurements described here were performed at the ISIS Rutherford Appleton Laboratory on the ENGIN-X instrument [16], which is one of the few facilities capable of handling such large and heavy samples. ENGIN-X is a time-of-flight facility using a spallation neutron source, so multiple diffraction peaks can be obtained simultaneously. This enables the lattice spacing to be obtained directly using a Rietveld refinement of a time of flight profile; this is carried out using GSAS software [17].

Collimators on the incident and detected beams allow the user to define a small 'gauge volume' for each measurement; in this case a 4×4×4mm cube. Samples are mounted on a numerically-controlled table which can be positioned so that the desired region of the sample is within the measured gauge volume. The SScanSS software [20],[21] can be used to simulate the tests, prepare numerical scripts to position the samples, and to predict the neutron beam path length through the wheel, and hence the time required to achieve a clear diffraction spectrum.

In this experiment, the wheels were mounted vertically when measuring radial and axial strains (Figure 2a) and at an elevation of 20° from the horizontal for the hoop strains (Figure 2b). Previous experiments [11] used a 60° elevation for the hoop strain measurements, favouring measurements across the tread surface at the expense of measurements through the depth of the rim.

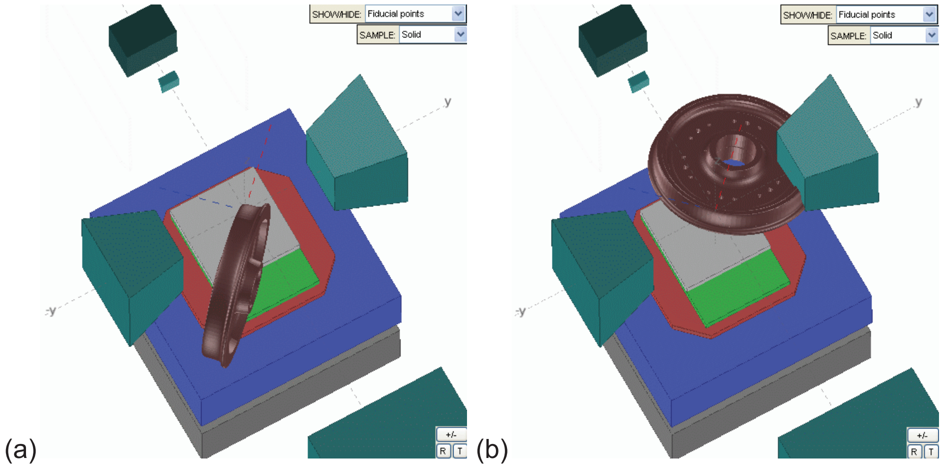

Figure 2: (a) Wheel orientation for measurement of radial and axial strains shown in SScanSS simulation. The incident beam approaches from the upper left, and measurements of neutrons reflected at 90° indicate the strain in the direction bisecting that angle. The radial strain (red dotted line) is measured in bank 1 (right) and the axial strain (blue dotted line) in bank 2 (left). (b) Wheel orientation for measurement of hoop strain. Note that this orientation (positioned at 20° from the horizontal) requires the removal of the bank 1 collimator; the hoop strain measurements are made in bank 2 (left).

Methodology: Measurement Points

Although neutron diffraction is one of the most penetrative non-destructive techniques for strain measurement, there are practical limitations on the regions of the wheel that can be tested. For steel samples tested on ENGIN-X, the relationship between the path length in mm and the minimum test time in minutes is as follows:

$$\text{time} = 0.2229 \times e^{(0.1146 \times \text{path length})}$$

The low rate of neutrons reaching the detector for longer path lengths mean that these measurements are more affected by ‘noise’ from randomly scattered neutrons.

Figure 3 indicates the total test time to achieve the axial/radial and hoop strain measurements at each point in the wheels, ignoring any set-up time for the different wheel orientations. If the total time to measure the 3 strain components at a single point is over 24 hours, this is shown in black and may be considered impractical. On the new and mid-life wheels, the measurable regions are limited to the flange and the field side regions near the tread (running) surface or rim face. In practice, these wheels rarely suffer any failures in the flange so the stresses in that region are of less interest.

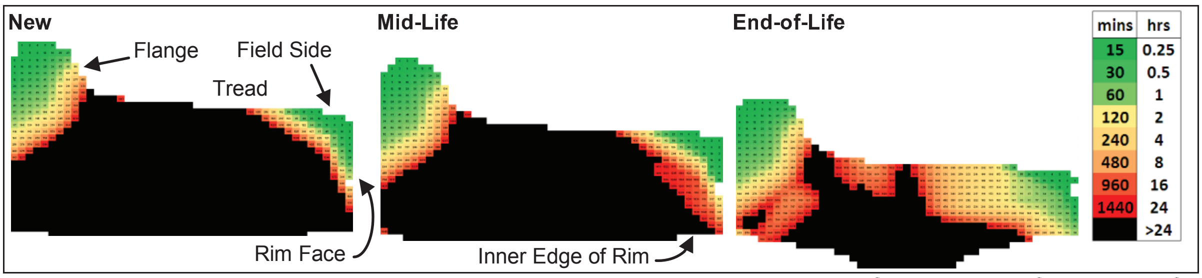

Figure 3: Time to measure all three principal strains at a location in the wheel rim, for New, Mid-Life and End-of-Life wheels. Regions of the wheel are annotated for reference in the subsequent description.

The end-of-life wheel presents quite a different picture to the other two, because there are plausible path lengths for hoop strain measurements with the beam entering from the inner edge of the wheel rim. Using the shallow 20° elevation enables this approach, and the path length for radial strain measurements becomes the limiting factor in many areas of the rim. Even so, the total time for strain measurements at a single point toward the centre of the wheel rim is around 8 hours, strictly limiting the number of points that can be measured in a realistic beam-time allocation of a few days.

The measurement 'gauge volumes' on each sample were selected to optimise use of the available beam-time, and measured the field side region as far as practical through the depth of the rim.

Methodology: Determination of Stress-Free Lattice Parameter

The determination of residual stress from diffraction data is based on the difference between the lattice spacing in the stressed condition and the spacing in a stress-free condition. It is therefore important to know the stress-free lattice spacing (d_0) for the sample being considered [22]. Previous work by the authors has identified that the material properties within the wheel rim are anisotropic and inhomogeneous [5], with variations in ferrite fraction and plastic flow in the near-surface region.

It is plausible that the stress-free lattice spacing is influenced by these variations, so the d_0 was measured in all three principal directions (radial, axial and hoop) at locations across the rim using two 'comb' samples [22], with the comb teeth in axial and radial directions. Measurements were made to coincide with the planned gauge volumes in the entire wheels, plus a coarse grid across the remainder of the wheel rim to characterise any overall trends. The comb samples were cut from a wheel nearly identical to the entire mid-life wheel used in the main series of tests.

It was found that there are slight variations of d_0 with depth below the running surface, which may be related to the variations in the pro-eutectoid ferrite fraction and hardness within the wheel rim. Near-surface regions which may have been affected by plastic flow [5] also show variations in d_0. Most significantly, there were clear variations between the axial, radial and hoop d_0 values, suggesting that the stress-free lattice spacing is anisotropic. When calculating strains and stresses in the entire wheel measurements, the locally measured d_0 values were used.

Results

Radial, axial and hoop strains were measured in the gauge volumes. The hoop strain is the most significant and Figure 4(a) shows the variation of hoop strain through the depth of the wheel rim. The upper point on each line is just below the tread running surface. Where more than one gauge volume was measured at a given depth (usually near the running surface) then the result shown is an average for that depth.

All the hoop strains are significantly compressive and tend to increase with depth. The two used wheels show a reversal of this trend near the running surface of the wheel where significant plastic flow is present. Error magnitudes output from the Rietveld refinement software [17] are also shown; these are relatively small compared to the absolute values of strain.

(a) (b)
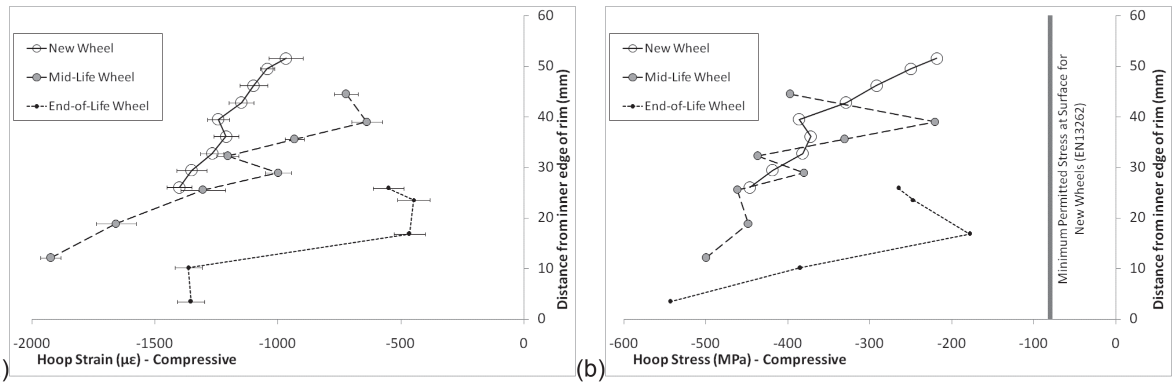

Figure 4 (a) Residual hoop strain through the depth of the wheel rims, showing error magnitudes calculated by GSAS; (b) Residual hoop stress through the depth of the wheel rims, calculated from all three strain components.

Figure 4(b) shows the variation of hoop stress with depth; this is calculated from the radial, axial and hoop strains. The influence of the other strain components changes the trends slightly but the overall pattern remains similar. At all points measured, the hoop stresses are negative and exceed the minimum limit for hoop stress at the running surface defined in EN13262 [6].

Assuming that the as-manufactured stress distribution was similar for all three wheels, the stresses are redistributed within the wheel rim during its life as material is removed and plastic flow occurs. However, the hoop stress near the running surface remains compressive. Running in service appears to increase the compressive hoop stress in the near-surface regions. In the field-side region of the wheel (which overhangs the wheel web), the compressive hoop stresses may be reacted by shear stresses that are not measured using this method.

CONCLUSIONS

Neutron diffraction techniques can be used to measure the distribution of strains and stresses in entire railway wheels, but practical path-length limitations mean that they cannot reach the middle of the wheel rim. These measurements were therefore limited to the field side region of the wheel which may not be representative of the wheel as a whole.

Measurements of the stress-free lattice spacing d_0 using comb samples indicated that this parameter is significantly anisotropic, and can also vary with position in the wheel rim.

Assuming that the as-manufactured stress distribution was similar for all three wheels, the stresses are redistributed within the wheel rim during its life as material is removed (through in-service wear and turning on a wheel lathe) and plastic flow occurs. However, the hoop stress near the running surface remains compressive, typically in the range 200MPa to 400MPa. This exceeds the minimum limit for hoop stress at the running surface defined in EN13262.

The authors now intend to assess the significance of axial, radial and shear stresses in the wheels, and to compare the neutron diffraction results to those from the ultrasonic and destructive methods, combined with finite element modelling.

ACKNOWLEDGEMENTS

Experiments at the ISIS Pulsed Neutron and Muon Source were supported by a beamtime allocation from the Science and Technology Facilities Council. The authors would also like to acknowledge the support received from the Rail Safety and Standards Board, Siemens, Lucchini UK, Rail Research UK Association and EPSRC.

REFERENCES

[1] Bevan, A., Molyneux-Berry, P., ‘*Train Architecture and Operational Parameters Evaluation to Optimise Wheel Damage Control for Operators: Final Summary Report’*, RSSB Project T963-01, May 2013.

[2] Molyneux-Berry, P., Bevan, A., ‘*Wheel surface damage: relating the position and angle of forces to the observed damage patterns’*, IAVSD Conference, Manchester, 2011.

[3] Ekberg, A., Akesson, B., Kabo, E., ‘*Wheel/Rail rolling contact fatigue – probe, predict, prevent’*, 9th International Conference on Contact Mechanics and Wear of Rail/Wheel Systems (CM2012), Chengdu, August 27-30, 2012.

[4] Bernasconi, A., Davoli, P., Filippini, P., Foletti, S., *‘An integrated approach to rolling contact sub-surface fatigue assessment of railway wheels’*, Wear 258 (2005) 973–980

[5] Molyneux-Berry, P., Davis, C.L., Bevan, A., ‘*The Influence of Wheel/Rail Contact Forces on the Material Properties of Wheels in Service*’, 9th International Conference on Contact Mechanics and Wear of Rail/Wheel Systems (CM2012), Chengdu, China, August 27-30, 2012.

[6] ‘*Railway applications - Wheelsets and bogies - Wheels - Product Requirements’*, BS EN 13262:2004 +A2:2011

[7] *‘Railway rolling stock materials - Part 3: Specification for monobloc wheels for traction and trailing stock’*, BS 5892-3:1992+A2:2009

[8] Diener, M., Ghidini, A., ‘*Reliability and safety in railway products: fracture mechanics on railway solid wheels’*, Lucchini RS, 2008.

[9] KLW, *‘Wheels and Tyres for Railways’*, http://www.interpipe.biz/files/Wheels-PDF_2009.pdf

[10] *‘Advanced Forging Technologies, Heat Treatment for Railway Wheels, Tyres and Rings’*, http://www.presstrade.com/downloads/aft/AFT_WBER_E.pdf

[11] Alessandroni, M., Paradowska, A.M., Perelli Cippo, E., Senesi, R., Andreani, C., Gorini, G., Montedoro, P., Chiti, F., Sala, D., Spinelli, D., ‘*Investigation of Residual Stress Distribution of Wheel Rims using Neutron Diffraction*’, Materials Science Forum Vol 681 (2011) 522-526

[12] Mutton, P., Lynch, M.R., ‘*Improving the safety of railway wheels through nondestructive measurement of residual stresses’*. In: Proceedings of Conference on Railway Engineering , 2004,.Darwin.

[13] Bouchard, J., ‘*Advances in the Contour Method’*, IMechE Conference: ‘Residual Stress Engineering: Developing Control, Measurement and Characterisation Techniques’, Manchester, January 2013

[14] Linamanaik, S.N., Chen, B.K., ‘*Thermo-mechanical modelling of residual stresses induced by martensitic phase transformation and cooling during quenching of railway wheels*’, Journal of Materials Processing Technology 211, 2011.

[15] Gordon, J., Perlman, B., ‘*Estimation of residual stresses in railroad commuter car wheels following manufacture*’, FRA report DOT/FRA/ORD-03/24, 2003.

[16] Oliver, E., Santisteban, J., James, J., Daymond, M., Dann, J., ‘*ENGIN-X User Manual’*, ISIS & Open University, 16 August 2004

[17] Larson, A.C., Von Dreele, R.B., ‘*General Structure Analysis System (GSAS)*’, Los Alamos National Laboratory Report LAUR 86-748 (2004).

[18] Evans, A., ‘*Neutrons for non-destructive residual stress characterisation for rail applications’*, IOM3 Conference, York, 2011

[19] Grosse M., Ottlinger, P., ‘*Strain measurements at railway wheels*’, Materials Science and Engineering A 437 (2006) 88–92

[20] James, J., Santisteban, J., Edwards, L., Daymond, M., ‘*A Virtual Laboratory for Neutron and Synchrotron Strain Scanning*’, Physica B, Condensed Matter (2004) 350 pp.743-746.

[21] James, J., Edwards, L., ‘*Application of robot kinematics methods to the simulation and control of neutron beam line positioning systems*’, Nuclear Instruments and Methods in Physics Research A. (2007) 571, 709-718

[22] Withers, P. J., Preuss, M., Steuwerb, A., Pangc, J. W. L., ‘*Methods for obtaining the strain-free lattice parameter when using diffraction to determine residual stress*’, Journal of Applied Crystallography, (2007). 40, 891–904